Generation of Nitrile *N*-Sulfide (RCNS) Radical Cations and Neutrals via Ion−Molecule Reactions: Tandem Mass Spectrometry and ab Initio MO Study

Pascal Gerbaux, Yves Van Haverbeke, and Robert Flammang*

Organic Chemistry Department, University of Mons-Hainaut, Avenue Maistriau 19, B-7000 Mons, Belgium

Ming Wah Wong* and Curt Wentrup*

Department of Chemistry, The University of Queensland, Brisbane, QLD 4072, Australia

Received: April 3, 1997; In Final Form: June 30, 1997⊗

Electron impact ionization of carbon disulfide at a pressure of ca. 0.5−1 Torr generates $CS_2^{\bullet+}$ together with a variety of other sulfur-containing ions dominated by $CS_3^{\bullet+}$ and $C_2S_2^{\bullet+}$ radical cations (5 and 1% of the intensity of the CS_2 (*m*/*z* 76) base peak, respectively). The $CS_3^{\bullet+}$ ions were found to be efficient agents for $S^{\bullet+}$ transfer to the nitrogen atom of nitriles, thus yielding nitrile *N*-sulfide radical cations, $RCNS^{\bullet+}$ (R = H, CH_3, C_2H_5, C_3H_7, C_6H_5, Cl, Br, and I). These reactions were performed in a chemical ionization source and also in an RF-only quadrupole collision cell installed in the middle of a six-sector tandem mass spectrometer (EBEEBE). The connectivity of the $RCNS^{\bullet+}$ ions is established by collisional activation, and the stability of the corresponding neutral molecules is evaluated by the neutralization−reionization technique. The structures and energies of $CS_3^{\bullet+}$, $RCNS^{\bullet+}$, and neutral RCNS (R = H, Br, CH_3 and C_6H_5) were examined by G2(MP-2,SVP) theory. The calculated stabilities of the RCNS neutrals and the fragmentation energies of the $RCNS^{\bullet+}$ radical cations are in good accord with experimentally observed fragmentation patterns.

Introduction

Nitrile sulfides, R−C≡N→S, are little-known reactive intermediates.[1] The methyl and phenyl derivatives have been investigated by matrix isolation IR spectroscopy in conjunction with flash vacuum thermolysis (FVT),[2] but the parent compound, HCNS, has been observed only by mass spectrometry, including neutralization−reionization (NR) mass spectrometry.[1b,2] The NRMS technique has also permitted the identification of several new nitrile sulfides, generated by dissociative ionization of 1,2,5-thiadiazoles.[3] Moreover, we have recently discovered a novel method of generating nitrile sulfides, viz. sulfur transfer from $CS_3^{\bullet+}$ to nitriles, a technique that promises to be of value for the generation of a wide variety of new sulfur-containing species (*N*-sulfides, *S*-sulfides, etc). In this paper we are pleased to report experimental details of the method and its use in the generation and characterization of nitrile sulfides.

Experimental Section

The spectra were recorded on a large-scale tandem mass spectrometer (Micromass AutoSpec 6F) combining six sectors of EBEEBE geometry (E stands for electric sector and B for magnetic sector).[4] General conditions were 8 kV accelerating voltage, 1 mA emission current, 70 eV ionizing electron energy, and 200 °C ion source temperature.

In the chemical ionization (CI) experiments, 2−3 μL of CS_2 were injected via a septum, giving a pressure of ca. 10^{-5} Torr in the source housing and an estimated pressure of 0.5−1 Torr in the CI cell. The nitrile samples (ca. 1 μL) were also introduced into the CI source via the heated (180 °C) septum inlet.

The CA and NR spectra were recorded by scanning the field of the third electric sector and recording the fragments with an off-axis photomultiplier detector in the fifth field-free region. Oxygen collision gas was used in these experiments at a pressure appropriate to reduce the intensity of the mass-selected ion beams by ca. 30%. In the NR experiments, the reionization step was preceded by neutralization with ammonia (also 70% transmittance), unreacted ions being removed by floating the intermediate calibration ion source at 9 kV.

Recently, we have modified the tandem mass spectrometer for the study of associative ion−molecule reactions. Briefly, an RF-only quadrupole collision cell (the "Qcell") is inserted in the field-free region separating MS1 (EBE) and MS2 (EBE; Figure 1).[5] With this cell floated at ca. 7995 V, a beam of ions (8 keV) selected by MS1 is decelerated to 5 eV before entering the gas cell. Under these conditions, the probability of ion−molecule reactions is enhanced, but *not* that of collision-induced dissociations.[5] The pressure in the Qcell is estimated as 10^{-3} Torr. The ion−molecule products, reaccelerated at 8 keV, can then be separated by MS2 by scanning the field of the magnetic sector (B scan). Moreover, the high-energy CA spectra of the ions present in the quadrupole cell can be recorded by a linked scanning of the last three sectors (EBE; resolved mode) or a conventional scanning of the field of the last electric sector (ESA4) after mass selection with the second magnet.

Results and Discussion

1. Self-CI Reactions of CS_2. Several ions are produced in the source during the self-chemical ionization of carbon disulfide. The relative abundances of these ions are collected in Table 1 together with their structures proposed on the basis of the collisional activation (CA) spectra. The lighter ions ($S^{\bullet+}$ and $CS^{\bullet+}$) are the products of unimolecular dissociations, while others must be produced in ion−molecule reactions. By using the quadrupole reaction cell (Qcell), it is possible to investigate their mechanisms of formation (Scheme 1).

The reaction between $CS_2^{\bullet+}$ and CS_2 in the Qcell leads to the formation of *m*/*z* 88, 108, and 152 ions (intensity ratio 1.5:8:1). The CA spectrum of the *m*/*z* 152 ions indicates that these ions give rise to two other fragment ions (*m*/*z* 88 and 108). In

---

⊗ Abstract published in *Advance ACS Abstracts,* August 15, 1997.

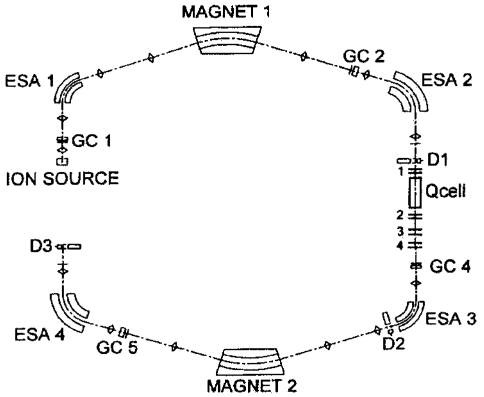

Figure 1. Schematic representation of the AutoSpec 6F mass spectrometer in the hybrid configuration with added Qcell. ESA = electrostatic analyzer. 1: deceleration lenses; 2: acceleration lenses; 3: *Y*/*Z* lenses; 4: demagnification lenses. GC = gas cell. D = off-axis detector. Qcell = quadrupolar cell.

TABLE 1: Self-CI Mass Spectrum of Carbon Disulfide

m/*z*	species	relative intensity (%)	connectivity[a]
32	S	5	
44	CS	11	
64	S_2	2	
76	CS_2	100	$S{=}C{=}S^{\bullet+}$
88	C_2S_2	1	$S{=}C{=}C{=}S^{\bullet+b}$
96	S_3	<1	
108	CS_3	5	$S{=}C{=}S{-}S^{\bullet+}$, $SC(S)S^{\bullet+}$
120	C_2S_3	<1	$S{=}C{=}C{=}S{-}S^{\bullet+}$
140	CS_4	<1	$S{=}C{=}S{-}S{-}S^{\bullet+}$
152	C_2S_4	<1	
160	S_5	<1	
192	S_6	<1	

[a] Connectivities proposed on the basis of the CA spectra. [b] Cf.: (a) Sülzle, D.; Schwarz, H. *Angew. Chem., Int. Ed. Engl.* **1988**, *27*, 10. (b) Wentrup, C.; Kambouris, P.; Evans, R. A.; Owen, D.; Macfarlane, G.; Chuche, J.; Pommelet, J. C.; Ben Cheikh, A.; Plisnier, M.; Flammang, R. *J. Am. Chem. Soc.* **1991**, *113*, 3130. (c) Maier, G.; Reisenauer, H. P.; Schrot, J.; Janoschek, R. *Angew. Chem., Int. Ed. Engl.* **1990**, *29*, 1464. (d) Wong, M. W.; Wentrup, C.; Flammang, R. *J. Phys. Chem.* **1995**, *99*, 16949.

SCHEME 1

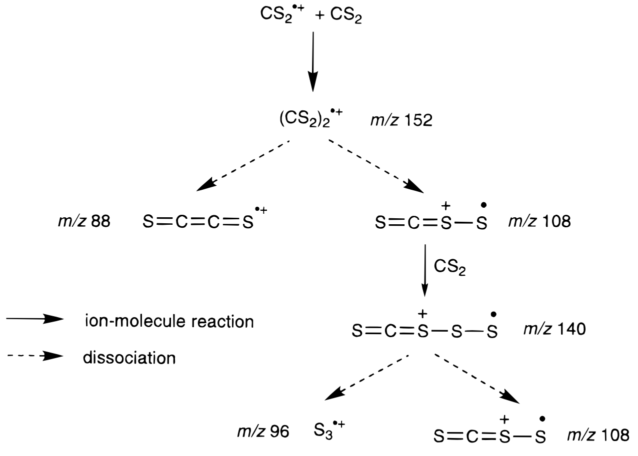

SCHEME 2

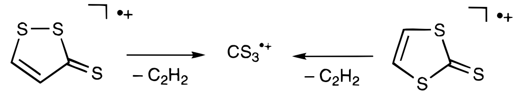

1 **2**

TABLE 2: Calculated Structural Parameters for H−C≡N−S[a]

level	r(C−N)	r(H−C)	r(N−S)	∠HCN	∠CNS
MP2/6-31G*	1.192	1.068	1.591	161.1	176.3
MP2/6-31+G*	1.195	1.070	1.586	158.2	175.8
MP2/6-311G**	1.185	1.064	1.590	179.9	180.0
MP2/6-311+G**	1.191	1.066	1.582	162.8	176.4
MP2/6-311+G(2d,p)	1.180	1.064	1.594	176.9	179.4
MP2/6-311+G(2df,p)	1.181	1.064	1.581	177.0	179.5
MP2/6-311+G(3df,2p)	1.182	1.062	1.578	177.2	179.5
MP2/CC-pVDZ	1.200	1.077	1.598	161.3	176.3
MP2/CC-pVTZ	1.182	1.061	1.586	177.9	179.6

[a] Bond lengths in angstroms and angles in degrees.

TABLE 3: Calculated Relative Energies (kJ mol^{-1}) of CS_3 Radical Cations and Fragments[a,b]

species[c]	symmetry	state	relative energy
$SCSS^{\bullet+}$ (**3**)	C_s	$^2A''$	0.0
$CS_3^{\bullet+}$ (**4**)	C_{2v}	$^2A_2$	42.4
$CS_3^{\bullet+}$ (**5**)	C_{2v}	$^2B_2$	46.3
$CS_3^{\bullet+}$ (**6**)	C_{2v}	$^2B_1$	125.4
$CSSS^{\bullet+}$ (**7**)	C_{2v}	$^2B_1$	262.8
$CS + S_2^{\bullet+}$ (*m*/*z* 64)			204.6
$^1S + CS_2^{\bullet+}$ (*m*/*z* 76)			372.1
$CS_2 + S^{\bullet+}$ (*m*/*z* 32)			454.3
$S_2 + CS^{\bullet+}$ (*m*/*z* 44)			468.9

[a] G2(MP2,SVP) E_0 values. [b] Calculated G2(MP2,SVP) E_0 energies include −1 230.880 88 ($SCSS^{\bullet+}$, **3**), −833.524 22 (CS_2), −833.153 19 ($CS_2^{\bullet+}$), 795.432 88 (S_2), −795.411 404 ($S_2^{\bullet+}$), 435.706 56 (CS), −435.287 03 ($CS^{\bullet+}$), −397.603 60 (S) and −397.201 25 ($S^{\bullet+}$) hartrees. [c] ^1S denotes the singlet state of the sulfur atom.

addition, *m*/*z* 140 ions ($CS_4^{\bullet+}$) are produced during the reaction between CS_2 and $CS_3^{\bullet+}$. The collisional activation spectrum of the *m*/*z* 140 ions demonstrates that they can undergo dissociations leading to the formation of the *m*/*z* 108 and 96 ions.

The most important ion−molecule reaction product is the *m*/*z* 108, $[C,S_3]^{\bullet+}$ radical cation (Table 1 and Scheme 1). The CA spectrum[7] suggest the carbon disulfide *S*-sulfide connectivity, SCSS, but a similar pattern can also be expected for the isomeric carbon trisulfide, SC(S)S. In fact, very similar CA spectra of the $CS_3^{\bullet+}$ ions are obtained upon dissociative ionization of the isomeric dithiolethiones **1** and **2** (loss of ethyne; Scheme 2),[8] as confirmed by our own measurements. This may be indicative of the occurrence of a mixture of isomers in these experiments, or that both isomers rearrange to the more stable $S{=}C{=}S{-}S^{\bullet+}$ (see section 6 and Table 3).

The neutralization−reionization spectrum[7] of $CS_3^{\bullet+}$ presents a significant recovery signal and fragmentations in keeping with those observed in the CA spectrum. The increased intensity of the *m*/*z* 44 and 64 peaks in the NRMS indicates that neutral CS_3 undergoes partial fragmentation to CS and S_2 in the neutralization cell.

2. Sulfuration of Nitriles. Chemical ionization of acetonitrile using CS_2 as the reagent gas leads to the formation of *m*/*z* 73 ions $[C_2H_3NS]^{\bullet+}$. The CA spectrum of these ions is shown in Figure 2a. The peaks at *m*/*z* 58 (loss of $CH_3^{\bullet}$) and 32 ($S^{\bullet+}$) are indicative of the acetonitrile *N*-sulfide connectivity, $CH_3{-}C{\equiv}N^+{-}S^{\bullet}$. The peaks at *m*/*z* 47, 46, 45 must arise from rearrangement processes. In fact, the best indication for the CCNS connectivity is found in the analysis of the CA spectra of the molecular ions of methyl thiocyanate and methyl isothiocyanate which display very different fragmentation patterns.[2] Moreover, an intense charge stripping peak (*m*/*z* 36.5; CH_3CNS^{2+}) is observed only for the $CH_3CNS^{\bullet+}$ ions, a situation frequently found for α-distonic radical cations,[9] where the positive charge and the radical are located on different atoms (see also section 4).

The neutralization−reionization spectrum of these *m*/*z* 73 ions (Figure 2b) features an intense recovery signal and fragments

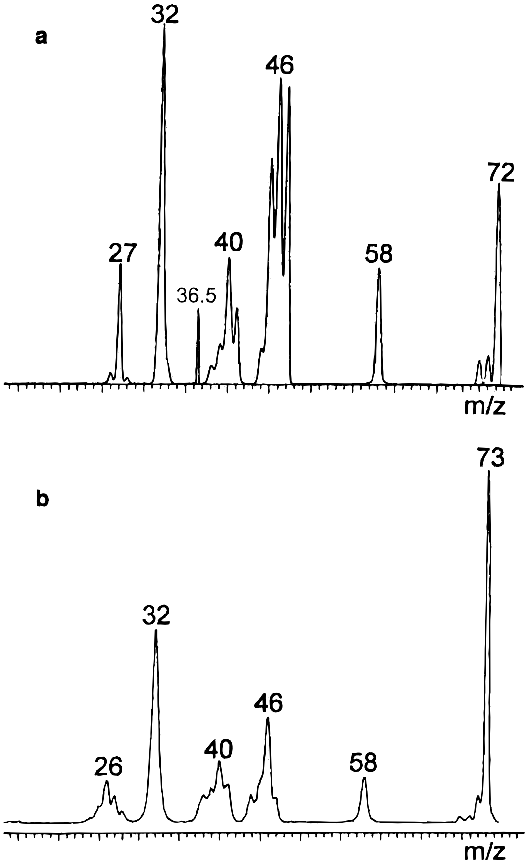

Figure 2. (a) CA (O_2) and (b) NR (NH_3/O_2) mass spectra of the *m/z* 73 ions ($CH_3CNS^{\bullet+}$) generated by sulfuration of acetonitrile under CI (CS_2) conditions (the signal at *m/z* 36.5 is due to charge stripping to CH_3CNS^{2+}). The ordinates are intensity in arbitrary units in all the MS figures.

SCHEME 3

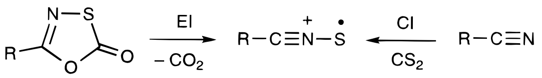

quite similar to those observed in the CA spectrum, except for *m/z* 47 which is ascribed to a rearrangement process not favored when high internal energy is conferred on the ions.[10] The absence of charge stripping (*m/z* 36.5) in the NR spectrum is not unprecedented and is presumably due to the low probability of an m → m^{2+} double ionization.[10c,11] The high intensity of the recovery signal indicates the stability of the neutral acetonitrile *N*-sulfide in the gas phase.

The sulfuration of HCN and other aliphatic nitriles (C_2H_5-CN and C_3H_7CN) has also been performed, with results analogous to those described for the sulfuration of acetonitrile. The HCN results support the previous identification of thiofulminic acid, $H-C\equiv N\rightarrow S$, in the gas phase by neutralization of the corresponding ion.[2] Very similar CA and NR spectra are obtained for the ions produced by dissociative ionization of 1,3,4-oxathiazole-2-one (Scheme 3, R = H) and by sulfur transfer to HCN under the CI (CS_2) conditions.

The production of benzonitrile *N*-sulfide radical cation and neutral by dissociative ionization or flash vacuum pyrolysis of several heterocycles, including 5-phenyl-1,3,4-oxathiazole-2-one (Scheme 3, R = C_6H_5), has been reported elsewhere.[12] The direct sulfuration under chemical ionization conditions is a facile and rapid means of generating $Ph-C\equiv N^+-S^\bullet$ radical cations. The relevant CA and NR spectra are shown in Figure 3 and are identical with those obtained by fragmentation of heterocycles.[12] The intense peaks at *m/z* 103 (loss of S) and *m/z* 77 ($C_6H_5^+$) are indicative of the *N*-sulfide connectivity, and the observation of a very intense recovery signal in the NR spectrum is in keeping with the stability of the corresponding neutral in the gas phase.

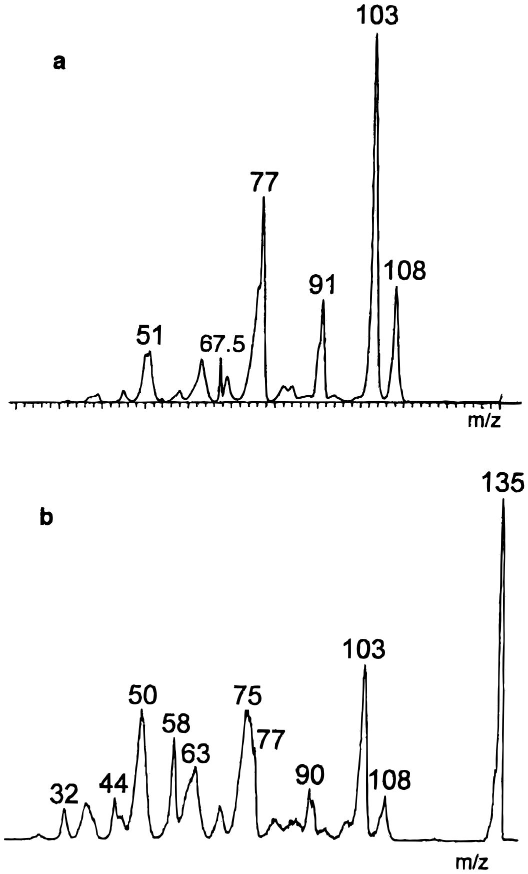

Figure 3. (a) CA (O_2) and (b) NR (NH_3/O_2) mass spectra of the *m/z* 135 ions ($PhCNS^{\bullet+}$) generated by sulfuration of benzonitrile under CI (CS_2) conditions.

3. Sulfuration of Cyanogen Halides. Three cyanogen halides (ICN, BrCN, and ClCN) were studied in a similar manner. The common behavior under the CI conditions is illustrated with the case of cyanogen bromide. The CA spectrum (Figure 4a) is again characteristic of the BrCNS connectivity: the major peaks are readily interpreted in terms of simple cleavage reactions with one notable exception, the loss of $CN^\bullet$ (*m/z* 111), which requires a rearrangement. The NR spectrum (Figure 4b) exhibits a strong recovery signal at *m/z* 137 and the expected decreased intensity of the peak due to rearrangement (*m/z* 111). The higher abundance of the Br^+ ions is due to reionization of bromine atoms generated in the neutralization cell.

The results for ClCNS were as previously reported.[3] For ICNS, the fragmentations (CA) are very similar to those of BrCNS and ClCNS, but in this case, the base peak is *m/z* 127 (I^+). In fact, in the XCNS series, the intensity of X^+ is inversely proportional to the electronegativity of the halogen: 7% (Cl), 20% (Br), and 100% (I). The other peaks for ICNS are at *m/z* 159 (loss of CN; rearrangement), *m/z* 143 (loss of S), *m/z* 139 (loss of NS), and *m/z* 58 (CNS^+). The NR spectrum is very similar to the CA spectrum, except for a significant decrease of *m/z* 159, which suggests that this is indeed due to a rearrangement reaction. The recovery signal for ICNS (*m/z* 185) is also intense: about 40% of the base peak (*m/z* 127).

4. Ion−Molecule Reactions. Figure 5a shows the result of a B scan (see Experimental Section) where mass-selected $CS_3^{\bullet+}$ ions were allowed to react with neutral acetonitrile in

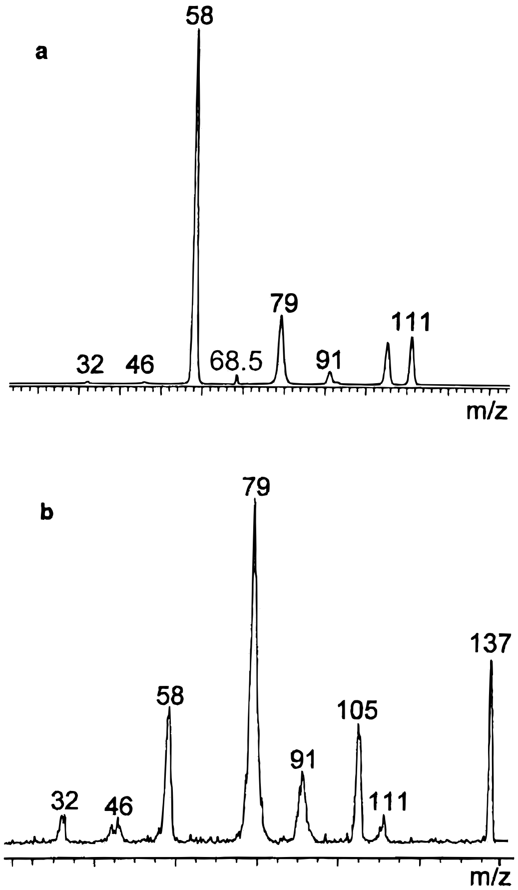

Figure 4. (a) CA (O_2) and (b) NR (NH_3/O_2) mass spectra of the *m/z* 137 ions ($^{79}BrCNS^{\bullet+}$) generated by sulfuration of cyanogen bromide (the signal at *m/z* 68.5 is due to charge stripping to $^{79}BrCNS^{2+}$).

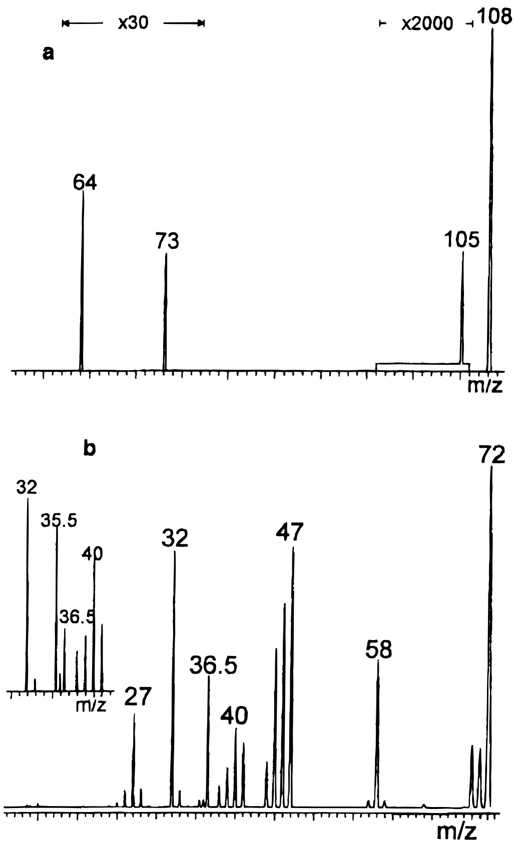

Figure 5. Reaction between mass-selected $CS_3^{\bullet+}$ radical cations and acetonitrile in the Qcell: (a) mass spectrum of the ions produced in the cell (B scan), and (b) CA (O_2) mass spectrum of the mass-selected *m/z* 73 ions ($CH_3CNS^{\bullet+}$) recorded in the linked scan mode. Inset: *m/z* 31−42 region for methyl isothiocyanate molecular ions, $CH_3-N{=}C{=}S^{\bullet+}$.

the quadrupolar cell. $[CH_3CN,S]^{\bullet+}$ ions (*m/z* 73) are clearly produced in these ion−molecule reactions. The *m/z* 64 ions ($S_2^{\bullet+}$) result from unimolecular decomposition of the $CS_3^{\bullet+}$ precursor ions (*m/z* 108). There is a very small amount of *m/z* 105 ions having the composition $[CH_3CN,S_2]$, which also lead to the $[CH_3CN,S]^{\bullet+}$ species: the CA spectrum is dominated by *m/z* 90 (loss of $CH_3^{\bullet}$) and 64 ($S_2^{\bullet+}$), but *m/z* 73 ($CH_3CNS^{\bullet+}$), 58 ($CNS^{\bullet+}$), and 46 ($NS^{\bullet+}$) are also observed. The likely structure is $CH_3CNSS^{\bullet+}$.

The principal advantage of the hybrid spectrometer is the ability to obtain collisional activation spectra (high energy) of mass-selected ion−molecule products in a field-free region of MS2. Figure 5b shows the CA spectrum (recorded in the linked scan mode) of the *m/z* 73 ions generated in the Qcell. The observed fragmentation pattern is identical with that described above under chemical ionization conditions (Figure 2a). The intense peak at *m/z* 32 again indicates a structure with a terminal sulfur atom. Ionized methyl isothiocyanate, $CH_3N{=}C{=}S^{\bullet+}$, can be readily excluded. The charge stripping peak for $CH_3CNS^{\bullet+}$ (*m/z* 36.5) is very intense and makes it possible to distinguish this ion from the isomeric isothiocyanate where the charge stripping spectrum is instead dominated by C_2HNS^{2+} ions (*m/z* 35.5; see inset in Figure 5b).[13]

Molecular Orbital Calculations

5. Computational Methods. Standard ab initio[14] and density functional[15] calculations were carried out with the GAUSSIAN 92/DFT series of programs.[16] The structures and energies of $CS_3^{\bullet+}$, $C_2S_4^{\bullet+}$, RCNS, and $RCNS^{\bullet+}$ (R = H, Br, CH_3, and C_6H_5) and related fragments were examined at the G2(MP2,SVP) level of theory.[17] This corresponds effectively to QCISD(T)/6-311+G(3df,2p)//MP2/6-31G* energies together with zero-point vibrational and isogyric corrections. Spin-restricted calculations were used for closed-shell systems, and spin-unrestricted ones for open-shell systems. The frozen-core approximation was employed for all correlated calculations. Harmonic vibrational frequencies and infrared intensities were computed using the B3-LYP formulation[18] of density functional theory, i.e., the Becke three-parameter exchange functional[15a] and the Lee−Yang−Parr correlation functional.[15b] The directly calculated B3-LYP/6-31G* frequencies were scaled by a factor of 0.9613 to account for the overestimation of calculated frequencies at this level of theory.[19]

It has been found previously that sulfur-containing compounds may require a large basis set to obtain reliable geometries. Here, we have examined the effect of basis set on the structure of HCNS at the MP2 level (Table 2). The predicted C−N and N−S bond lengths are rather similar for all the different basis sets considered. On the other hand, the calculated HCN bond angle is very sensitive to the basis set used. The optimized MP2/6-31G* structure is strongly bent, while the MP2/6-311G** is linear. Our best calculation (MP2/6-311+G(3df,-2p)) predicts the HCNS structure close to linearity. Reliable prediction of the HCNS structure requires at least a triple-ζ type basis set with d and f polarization functions (e.g., 6-311+G-(2df,p) or CC-pVTZ). Hence, for all the sulfur-containing species considered in this paper, we have also calculated their structures at the MP2/6-311+G(2df,p) level (Figures 6 and 7).

6. $CS_3^{\bullet+}$ Radical Cations. The various isomeric forms of CS_3 and $CS_3^{\bullet+}$ have been studied previously at the UHF/6-31G* + ZPVE level.[8] Here, we have reexamined these species at a

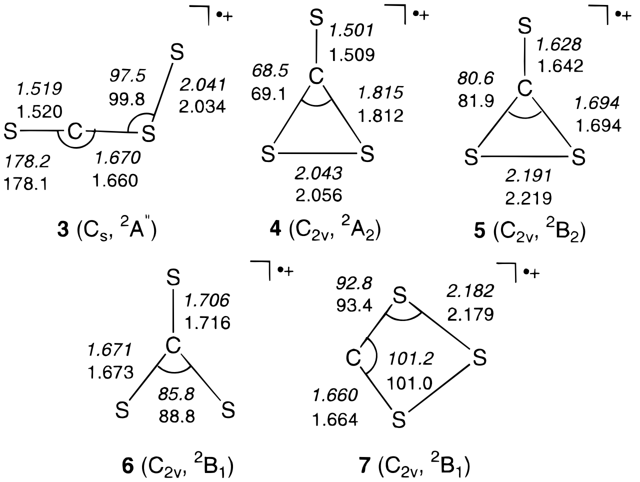

3 (C_s, $^2A''$) **4** (C_{2v}, $^2A_2$) **5** (C_{2v}, $^2B_2$)

6 (C_{2v}, $^2B_1$) **7** (C_{2v}, $^2B_1$)

Figure 6. Optimized geometries (MP2/6-31G*, with MP2/6-311+G(2df,p) values in italics) for equilibrium structures of CS_3 neutral and radical cation (bond lengths in angstroms and angles in degrees).

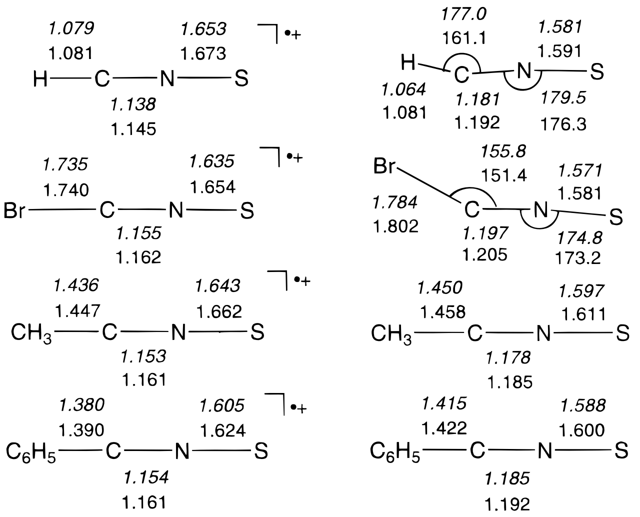

Figure 7. Optimized geometries (MP2/6-31G*, with MP2/6-311+G(2df,p) values in italics) of RCNS neutrals and radical cations (bond lengths in angstroms and angles in degrees).

TABLE 4: Calculated Relative Energies (kJ mol^{-1}) of RCNS Neutrals[a,b]

species[c]	relative energy	species[c]	relative energy
HCNS	0.0	CH_3CNS	0.0
CNSH	2.0	$CH_3CN + {}^1S$	245.0
HSCN	−122.0	$CH_3^\bullet + CNS^\bullet$	331.2
HNCS	−155.0	$H^\bullet + CH_2CNS^\bullet$	345.9
$HCN + {}^1S$	244.3	$CCH_3^\bullet + NS^\bullet$	926.7
$H^\bullet + CNS^\bullet$	345.5	C_6H_5CNS	0.0
$CH^\bullet + NS^\bullet$	606.9	$C_6H_5CN + {}^1S$	257.3
BrCNS	0.0	$C_6H_5^\bullet + CNS^\bullet$	410.8
$BrCN + {}^1S$	242.5	$CC_6H_5^\bullet + NS^\bullet$	580.0
$Br^\bullet + CNS^\bullet$	454.7		
$CBr^\bullet + NS^\bullet$	445.6		

[a] G2(MP2,SVP) E_0 values. [b] Calculated G2(MP2,SVP) E_0 energies include: −490.979 88 (HCNS), −3062.975 80 (BrCNS), −530.216 57 (CH_3CNS), and −721.598 82 (C_6H_5CNS) hartrees. [c] ^1S denotes the singlet state of the sulfur atom.

significantly higher level of theory, G2(MP2,SVP)[15] (Table 3). The carbon disulfide *S*-sulfide radical cation ($SCSS^{\bullet+}$, **3**) is predicted to be the global minimum on the $CS_3^{\bullet+}$ potential energy surface. This radical cation is best described as a *distonic radical ion*[9b] ($SCS^+S^\bullet$), where the charge and radical sites are formally separated.

There are three possible structures of carbon trisulfide radical cation with C_{2v} symmetry, $^2A_2$ (**4**), $^2B_2$ (**5**), and $^2B_1$ (**6**; Figure 6). All three C_{2v} forms are calculated to be local minima at the MP2/6-31G* level. The most stable of the C_{2v} structures corresponds to the $^2A_2$ (**4**) state, which has a S−S bond length close to that of a typical S−S single bond (Figure 6). The $^2B_2$ state (**5**) lies close in energy (4 kJ mol^{-1} above **4**) while the $^2B_1$ state (**6**) is significantly higher in energy (Table 3). However, the carbon trisulfide radical cation **4** is less stable than the ylide radical cation (**3**) by 42 kJ mol^{-1}. The D_{3h} form of $CS_3^{\bullet+}$ does not correspond to a local minimum on the $CS_3^{\bullet+}$ hypersurface. The four-membered ring structure (**7**) is predicted to be a stable equilibrium structure, but it lies 263 kJ mol^{-1} above **3**.

7. RCNS Neutrals. We have examined the structures and energies of four nitrile *N*-sulfides (RCNS), namely, HCNS, BrCNS, CH_3CNS, and C_6H_5CNS. All RCNS neutrals are calculated to be stable with respect to all possible unimolecular fragmentation processes (Table 4). Loss of a sulfur atom and loss of the R group are the most favorable dissociation pathways in all cases. Hence, these nitrile *N*-sulfides are confirmed as experimentally accessible and intrinsically stable species in the gas phase. For the parent thiofulminic acid (HCNS), the isomeric structures HSCN (thiocyanic acid) and HNCS (isothiocyanic acid) are predicted to lie 122 and 155 kJ mol^{-1}, respectively, below HCNS, while CNSH (isothiofulminic acid) is close in energy (2 kJ mol^{-1} above HCNS). There is little experimental evidence for HSCN, and none for HSNC, but there is one report on the possible existence of a derivative of HSNC.[18]

As with other nitrile sulfides,[3] HCNS and BrCNS are predicted to have a somewhat bent RCNS structure (Figure 7), but CH_3CNS and C_6H_5CNS are linear, which may be explained in terms of the effect of conjugation or hyperconjugation. As a consequence, the C−C bond lengths in CH_3CNS and C_6H_5CNS are very short, ca. 1.45 and 1.42 Å, respectively. As noted previously,[3] the p electrons in RCNS are delocalized in the CNS framework, as indicated by the somewhat longer C≡N triple bonds and shorter N−S bonds (Figure 7). The rather long N−S bonds suggest that these compounds are best approximated by the $R-C\equiv N^+-S^-$ resonance structure.

We have calculated the B3-LYP/6-31G* vibrational spectra of the nitrile *N*-sulfides. In agreement with previous findings,[3] the cumulenic CNS stretching frequency of RCNS depends strongly on the nature of the R substituent. The calculated (scaled)[19] CNS stretching frequencies for HCNS, BrCNS, CH_3CNS, and C_6H_5CNS are 2112, 2199, 2252, and 2216 cm^{-1}, respectively. The trend of calculated CNS frequencies is in accord with the trend of the calculated C≡N bond lengths in RCNS (Figure 7). For acetonitrile sulfide and benzonitrile sulfide, the calculated B3-LYP/6-31G* CNS frequencies are in reasonable accord with experiment (2230 and 2185 cm^{-1}, respectively).[2]

8. $RCNS^{\bullet+}$ Radical Cations. Consistent with the experimental findings, all the nitrile *N*-sulfide radical cations are predicted to be stable toward unimolecular fragmentation (Table 5). It is important to note that experimental CA spectra are composites of both collision-induced and unimolecular reactions, which may include rearrangement processes. Thus, a perfect correlation between observed ion intensities and calculated fragmentation energies is not to be expected. Nevertheless, the calculated fragmentation pattern of $HCNS^{\bullet+}$ agrees well with the relative intensities observed in the CAMS.[2]

For $BrCNS^{\bullet+}$, the experimental spectrum (Figure 4a) is in gross agreement with theoretical expectations. The CAMS is

TABLE 5: Calculated Relative Energies (kJ mol^{-1}) of RCNS Radical Cations[a,b]

species[c]	relative energy	species[c]	relative energy
$HCNS^{\bullet+}$	0.0	$CH_3CNS^{\bullet+}$	0.0
$HCN + S^{\bullet+}$ (*m/z* 32)	419.1	$H^{\bullet} + CH_2CNS^{+}$ (*m/z* 72)	312.1
$H^{\bullet} + CNS^{+}$ (*m/z* 58)	521.6	$CNS^{\bullet} + CH_3^{+}$ (*m/z* 15)	459.2
$CH^{\bullet} + NS^{+}$ (*m/z* 46)	554.5	$CH_3CN + S^{\bullet+}$ (*m/z* 32)	486.7
$^1S + HCN^{\bullet+}$ (*m/z* 27)	710.6	$NS^{\bullet} + CCH_3^{+}$ (*m/z* 27)	570.7
$NS^{\bullet} + CH^{+}$ (*m/z* 13)	748.8	$CH_3^{\bullet} + CNS^{+}$ (*m/z* 58)	574.1
$CNS^{\bullet} + H^{+}$ (*m/z* 1)	776.7	$^1S + CH_3CN^{\bullet+}$ (*m/z* 41)	611.1
		$CCH_3^{\bullet} + NS^{+}$ (*m/z* 46)	737.9
$BrCNS^{\bullet+}$	0.0	$CH_2CNS^{\bullet} + H^{+}$ (*m/z* 1)	844.0
$NS^{\bullet} + CBr^{+}$ (*m/z* 91)	431.2		
$CBr^{\bullet} + NS^{+}$ (*m/z* 46)	432.0	$C_6H_5CNS^{\bullet+}$	0.0
$BrCN + S^{\bullet+}$ (*m/z* 32)	456.0	$CNS^{\bullet} + C_6H_5^{+}$ (*m/z* 77)	372.3
$^1S + BrCN^{\bullet+}$ (*m/z* 105)	548.7	$^1S + C_6H_5CN^{\bullet+}$ (*m/z* 103)	388.9
$Br^{\bullet} + CNS^{+}$ (*m/z* 58)	669.5	$NS^{\bullet} + CC_6H_5^{+}$ (*m/z* 89)	450.7
$CNS^{\bullet} + Br^{+}$ (*m/z* 79)	829.6	$C_6H_5CN + S^{\bullet+}$ (*m/z* 32)	495.4
		$CC_6H_5^{\bullet} + NS^{+}$ (*m/z* 46)	591.0
		$C_6H_5^{\bullet} + CNS^{+}$ (*m/z* 58)	650.2

[a] G2(MP2,SVP) E_0 values. [b] Calculated G2(MP2,SVP) E_0 energies include −490.644 10 ($HCNS^{\bullet+}$), −3062.654 79 ($BrCNS^{\bullet+}$), −529.906 26 ($CH_3CNS^{\bullet+}$), and −721.287 20 ($C_6H_5CNS^{\bullet+}$) hartrees. [c] ^1S denotes the singlet state of the sulfur atom.

complicated by ions generated in rearrangement processes, in particular the signal at *m/z* 111 ($BrS^{\bullet+}$).

The calculated fragmentation energies of $CH_3CNS^{\bullet+}$ are in close agreement with the observed CAMS (Figure 2a). There are several peaks, e.g., *m/z* 47 ($CH_3S^{\bullet+}$), in the experimental spectrum which are attributed to rearrangements. As noted above, the *m/z* 47 peak is greatly reduced in the NR mass spectrum (Figure 2b).

For $C_6H_5CNS^{\bullet+}$, the agreement with experiment (Figure 3a) is good. Formation of $C_6H_5^{+}$ ions and loss of an S atom are the most favorable dissociation processes.

All $RCNS^{\bullet+}$ are calculated to be linear (Figure 7). The calculated C−N and N−S bond lengths in $RCNS^{\bullet+}$ and RCNS are similar. Since the HOMO of nitrile *N*-sulfides is dominated by the atomic p orbital on the S atom,[3] strong recovery signals are expected in the NR spectra, as is also observed in all cases.

Conclusions

Electron impact ionization of carbon disulfide at a pressure of ca. 0.5−1 Torr is a convenient source of $CS_3^{\bullet+}$ radical cations. On the basis of ab initio calculations, carbon disulfide *S*-sulfide ions ($S{=}C{=}S{-}S^{\bullet+}$) are expected to contribute significantly to the total population of the $CS_3^{\bullet+}$ ions. These ions react readily with nitriles, producing stable nitrile *N*-sulfide ions in reasonable yields. The stability of the corresponding neutrals in the gas phase is clearly established by neutralization−reionization experiments, confirming previous flash vacuum thermolysis results[2] (CH_3CNS and PhCNS). The calculated stabilities of RCNS neutrals and fragmentation energies of $RCNS^{\bullet+}$ radical cations support the identification of the stable nitrile *N*-sulfides.

Acknowledgment. The Fonds National de la Recherche Scientifique is acknowledged for a research fellowship for P. Gerbaux and for its contribution to the acquisition of the Micromass AutoSpec 6F mass spectrometer. The Brisbane laboratory thanks the Australian Research Council for financial support and for a research fellowship for M.W.W.

References and Notes

(1) (a) Paton, R. M. *Chem. Soc. Rev.* **1989**, *18*, 33−52. (b) Wentrup, C.; Kambouris, P. *Chem. Rev.* **1991**, *91*, 363−373.

(2) Kambouris, P.; Plisnier, M.; Flammang, R.; Terlouw, J. K.; Wentrup, C. *Tetrahedron Lett.* **1991**, *32*, 1487.

(3) Flammang, R.; Gerbaux, P.; Mørkved, E. H.; Wong, M. W.; Wentrup, C. *J. Phys. Chem.* **1996**, *100*, 17452.

(4) Bateman, R. H.; Brown, J.; Lefevere, M.; Flammang, R.; Van Haverbeke, Y. *Int. J. Mass Spectrom. Ion Processes* **1992**, *115*, 205.

(5) Flammang, R.; Van Haverbeke, Y.; Braybrook, C.; Brown, J. *Rapid Commun. Mass Spectrom.* **1995**, *9*, 795.

(6) (a) Delwiche, J. P.; Praet, M. *Adv. Mass Spectrom.* **1974**, *6*, 829. (b) Gress, M. E.; Linn, S. H.; Prest, H. F.; Ng, C. Y. *J. Chem. Phys.* **1980**, *72*, 4242. (c) Ono, Y.; Linn, S. H.; Prest, H. F.; Gress, M. E.; Ng, C. Y. *J. Chem. Phys.* **1981**, *74*, 1125.

(7) CA of $CS_3^{\bullet+}$: *m/z* 76 (85), 64 (100), 54 (3; M^{2+}), 44 (12), 32 (5%). NR of $CS_3^{\bullet+}$: *m/z* 108 (50), 76 (100), 64 (77), 44 (96), 32 (35%).

(8) Sülzle, D.; Egsgaard, H.; Carlsen, L.; Schwarz, H. *J. Am. Chem. Soc.* **1990**, *112*, 3750.

(9) (a) Holmes, J. L.; Lossing, F. P.; Terlouw, J. K.; Burgers, P. C. *Can. J. Chem.* **1983**, *61*, 2305. (b) Yates, B. F.; Bouma, W. J.; Radom, L. *J. Am. Chem. Soc.* **1986**, *108*, 6545.

(10) (a) Harnis, D.; Holmes, J. L. *Org. Mass Spectrom.* **1994**, *29*, 213. (b) Kuhns, D. W.; Tran, T. B.; Shaffer, S. A.; Turecek, F. *J. Phys. Chem.* **1994**, *98*, 4845. (c) Flammang, R.; Van Haverbeke, Y.; Wong, M. W.; Wentrup, C. *Rapid Commun. Mass Spectrom.* **1995**, *9*, 203. (d) Wong, M. W.; Wentrup, C.; Flammang, R. *J. Phys. Chem.* **1995**, *99*, 16849.

(11) Wiedman, F. A.; Cai, J.; Wesdemiotis, C. *Rapid Commun. Mass Spectrom.* **1994**, *8*, 804.

(12) (a) Maquestiau, A.; Flammang, R.; Plisnier, M.; Wentrup, C.; Kambouris, P.; Paton, M. R.; Terlouw, J. K. *Int. J. Mass Spectrom. Ion Processes* **1990**, *100*, 477. (b) Plisnier, M. Ph.D. Thesis, University of Mons-Hainaut, 1992.

(13) The loss of 2H (H_2) from the doubly charged $CH_3N{=}C{=}X^{2+}$ ions appears to be a dominant fragmentation for these cumulenic ions, but not for the isomeric CH_3CNX^{2+} ions; further theoretical and experimental work is in progress.

(14) Hehre, W. J.; Radom, L.; Schleyer, P. v. R.; Pople, J. A. *Ab Initio Molecular Orbital Theory*; Wiley: New York, 1986.

(15) (a) Parr, R. G.; Yang, W. *Density Functional Theory of Atoms and Molecules*; Oxford University Press: New York, 1989. (b) *Density Functional Methods*; Labanowski, J., Andzelm, J., Eds.; Springer: Berlin, 1991.

(16) Frisch, M. J.; Trucks, G. W.; Schlegel, H. B.; Gill, P. M. W.; Johnson, B. G.; Wong, M. W.; Foresman, J. B.; Robb, M. A.; Head-Gordon, M.; Replogle, E. S.; Gomperts, R.; Andres, J. L.; Raghavachari, K.; Binkley, J. S.; Gonzalez, C.; Martin, R. L.; Fox, D. J.; DeFrees, D. J.; Baker, J.; Stewart, J. J. P.; Pople, J. A. *GAUSSIAN 92/DFT*; Gaussian Inc.: Pittsburgh PA, 1992.

(17) (a) Smith, B. J.; Radom, L. *J. Phys. Chem.* **1995**, *99*, 6468. (b) Curtiss, L. A.; Redfern, P. C.; Smith, B. J.; Radom, L. *J. Chem. Phys.* **1996**, *104*, 5148.

(18) (a) Becke, A. D. *J. Chem. Phys.* **1993**, *98*, 5648. (b) Lee, C.; Yang, W.; Parr, R. G. *Phys. Rev. B* **1988**, *37*, 785.

(19) Wong, M. W. *Chem. Phys. Lett.* **1996**, *256*, 391.

(20) Christophersen, C.; Carlsen, P. *Tetrahedron Lett.* **1973**, 211.